Macromolecules

ARTICLE

pubs.acs.org/Macromolecules

Host−Guest Modulation of the Micellization of a Tetrathiafulvalene-Functionalized Poly(*N*-isopropylacrylamide)

Léna Sambe,[†,‡] François Stoffelbach,[§] Joel Lyskawa,[†,‡] François Delattre,[⊥] David Fournier,[†,‡] Laurent Bouteiller,[§] Bernadette Charleux,[∥] Graeme Cooke,[○,*] and Patrice Woisel[†,‡,▽,*]

[†]Université Lille Nord de France, F-59000 Lille, France

[‡]USTL, Unité des Matériaux Et Transformations (UMET, UMR 8207), Equipe Ingénierie des Systèmes polymères (ISP), F-59655 Villeneuve d'Ascq Cedex, France

[§]UMR 7610, Laboratoire de Chimie des Polymères, UPMC Université Paris 6—CNRS, 3, rue Galilée 94200 Ivry sur Seine, France

[⊥]UCEIV (Unité de Chimie Environnementale et Interactions sur le Vivant), EA 4492, Université du Littoral Côte d'Opale, Av. M. Schumann 59140 Dunkerque, France

[∥]CPE Lyon, CNRS UMR 5265, Laboratoire de Chimie Catalyse Polymères et Procédés (C2P2), Equipe LCPP Bat 308F, Université de Lyon, Université Lyon 1, 43 Bd du11 novembre 1918, F-69616 Villeurbanne, France

[○]Glasgow Centre for Physical Organic Chemistry, WestCHEM, School of Chemistry, University of Glasgow, Joseph Black Building, Glasgow, U.K., G12 8QQ, U.K.

[▽]ENSCL, F-59655 Villeneuve d'Ascq, France

Supporting Information

ABSTRACT: The aqueous solution properties of amphiphilic tetrathiafulvalene (TTF) end-functionalized poly(*N*-isopropylacrylamide) (PNIPAM) derivative **1** have been studied. Fluorescence spectroscopy, dynamic light scattering (DLS) and differential scanning calorimetry (Nano-DSC) were used to monitor the temperature-induced micellization and showed that **1** underwent two successive phase transitions corresponding to unimer-to-micelle and lower critical solution temperature (LCST) transitions, respectively. We have investigated the complexation properties of the TTF unit toward cyclobis(paraquat-*p*-phenylene) ($CBPQT^{4+}$) or the randomly methylated β-cyclodextrin (RAMEB) to manipulate the amphiphilicity of **1** and to control the unimer-to-micelle phase transition by forming pseudorotaxane-like architectures. For the RAMEB complex with **1**, the addition of a competitive guest such as 1-adamantanol resulted in the restoration of amphiphilicity of polymer **1** and consequently the reformation of micelles.

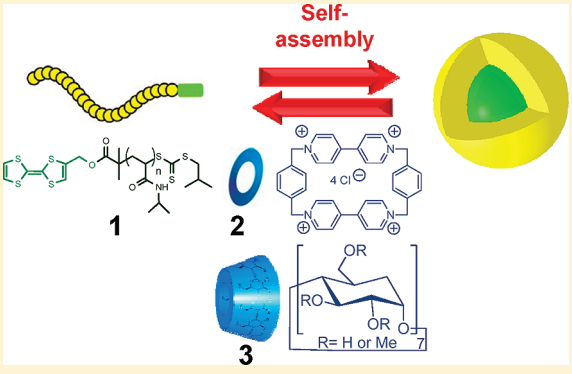

INTRODUCTION

The intersection of polymer science and supramolecular chemistry has led to the development of smart polymeric materials.[1−9] In particular, the rapidly developing field of supramolecular polymers has led to the development of sophisticated materials with interesting structures and functions.[10−17] The lock and key specificity of host−guest interactions offers the unique opportunity to control polymer structure (e.g., topology and morphology)[18−20] and properties (e.g., viscosity[21−23] and LCST[24,25]). Furthermore, the inherent reversibility of supramolecular architectures allows the modular and tunable modification of structure and properties of appropriately functionalized macromolecules.[26−30]

In the last decade, the development of polymeric micelles[31−35] has attracted considerable attention due to their unique properties such as the following: remarkably low critical aggregation concentration, unusual aggregation morphologies and their potential applications in nanoscience (e.g., nanocarriers,[36−40] nanoreactors[41]). Most of these micelle systems are fabricated from amphiphilic block copolymers upon contact with aqueous environments. Recent studies have highlighted the potential of using noncovalent interactions for modifying supramolecular polymer micelles (SMPMs),[42,43] with cyclodextrin (CD) being one of the most widely used hosts.[44,45] In particular, CDs have been exploited to trigger the amphiphilicity of block copolymers allowing the self-assembly of double hydrophobic[46] or hydrophilic block[47] polymers, or the disruption[48] or formation[49,50] of micelles. Host−guest interactions have also been exploited to construct

Received: May 2, 2011
Revised: July 4, 2011
Published: July 28, 2011

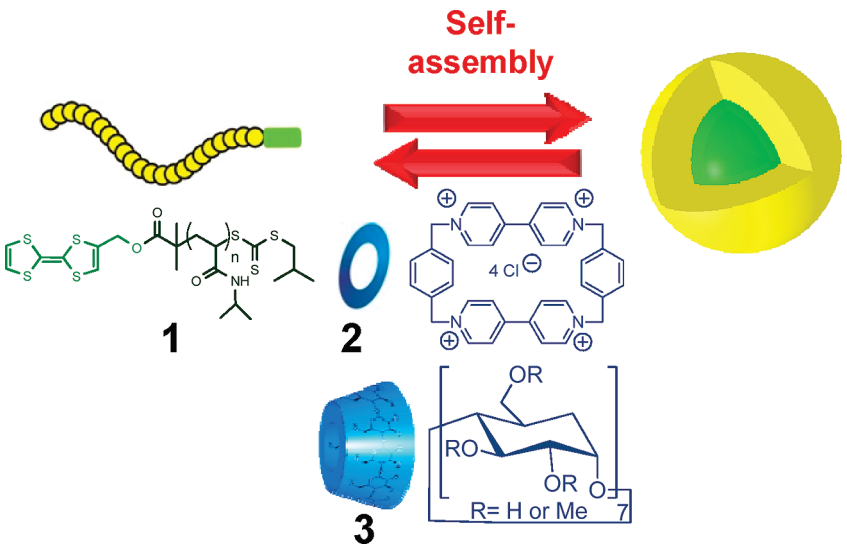

Figure 1. Schematic representation of the self-assembly of **1** and the structures of guests **2** and **3** used in this study.

supramolecular amphiphilic polymers from telechelic functionalized β-CD hydrophilic homopolymers and a short hydrophobic linker[51] or from two end decorated complementary hydrophobic and hydrophilic end functionalized homopolymers that can orthogonally self-assemble.[52,53]

It is clear that the application of host−guest complexation processes has provided a new impetus in micelle research, by allowing specific noncovalent interactions to modulate micelle self-assembly using convenient and tunable methodology. Understanding the role played by host−guest interactions in micellar self-assembly pathways may provide guidelines for the further development of micelles with applications including advanced materials and drug delivery systems. In a recent study, we have reported the synthesis of a new amphiphilic TTF end-functionalized PNIPAM homopolymer.[54] We have shown that amphiphilic homopolymers of this type can self-assemble in water affording a multistimuli responsive polymeric micelle. It is well-known that hydrophobic TTF unit is able of forming tunable pseudorotaxane assemblies with host molecules such as the electron-deficient tetracationic cyclophane **2**[55−57] or cyclodextrin[58] derivatives. In this work, we have exploited this virtue as a means to control and manipulate micelle formation. In particular, we have shown by fluorescence spectroscopy, dynamic light scattering (DLS) and differential scanning calorimetry (DSC) that the micellization process of **1** could be manipulated by forming pseudorotaxane assemblies with **2** and **3** (Figure 1). Furthermore, complexes formed between **1** and **3** can be then disrupted upon the addition of a competitive guest such as 1-adamantanol, thus allowing the reformation of micelles.

EXPERIMENTAL SECTION

Materials. Synthesis: **1**,[57] **2**,[59] and **4**[60] were prepared as previously described. Compound **3** and all reagents were purchased from Aldrich and were used as received.

Analytical Techniques. UV/vis turbidity measurements were carried out for lower critical solution temperature (LCST) determination using a Varian Cary 50 Scan equipped with a single cell Peltier temperature controller. Fluorescence spectra were recorded on a Perkin−Elmer LS 50B fluorescence spectrophotometer equipped with a single cell Peltier temperature controller. All electrochemical experiments were performed using an Autolab PGSTAT 30 workstation. A three electrode configuration was used with a platinum disk (2 mm diameter) as working electrode, an Ag/AgCl reference electrode, and a platinum wire as the counter electrode. The solution was purged with nitrogen prior to recording the electrochemical data, and all measurements were recorded at 15 °C under a nitrogen atmosphere. Dynamic light scattering experiments (DLS) were undertaken using a Malvern Zetasizer Nano ZS instrument using a light scattering apparatus equipped with a He−Ne (633 nm) laser and a thermoelectric Peltier temperature controller. The measurements were made at a scattering angle of 173° ("back scattering detection"). Dynamic light scattering (DLS) at 90° was undertaken with a Zetasizer Nano S90 from Malvern using a 5 mW He−Ne laser at 633 nm. The autocorrelation functions were analyzed with the CONTIN method. Thermograms were measured using a N-DSC III instrument from CSC at a scan rate of 0.5 °C/min. The reference cell was filled with degassed water and the sample cell (0.3 mL) with a degassed PNIPAM solution. The capillary cells were not capped, and a constant pressure of 6×10^5 Pa was applied. A baseline scan (water in both reference and sample cells) was performed in identical conditions and subtracted from the sample scan. Isothermal titration calorimetry (ITC) experiments were performed at 15 °C using a nano-ITC titration calorimeter from TA Instruments with a standard sample cell volume of 1 mL, following standard procedures. A 250 μL injection syringe was used with stirring at 400 rpm. Compound **1** was dissolved in deionized water and the solutions were degassed gently under vacuum before use. Each titration comprised an initial 1 μL preinjection followed by 25×10 μL injections of **3** (3 mM) into guest solution (0.2 mM). Control experiments with identical injections of **3** into water alone were used to correct titration data.

RESULTS AND DISCUSSION

The TTF-functionalized polymer **1** (M_n = 9730 g mol^{-1}, PDI = 1.14) was synthesized following previously reported procedures by reversible addition−fragmentation chain transfer (RAFT) polymerization.[54] The critical micelle concentration (CMC) of **1** in water was observed around 0.46 mg mL^{-1} at 24 °C by employing fluorescent dye solubilization methodology using Nile Red (NR) as fluorescence probe. As temperature is known to strongly affect the micellization process in aqueous phase, in this article, we have first investigated the influence of temperature on the micellization process of **1** by undertaking variable-temperature fluorescence experiments (Figure 2).

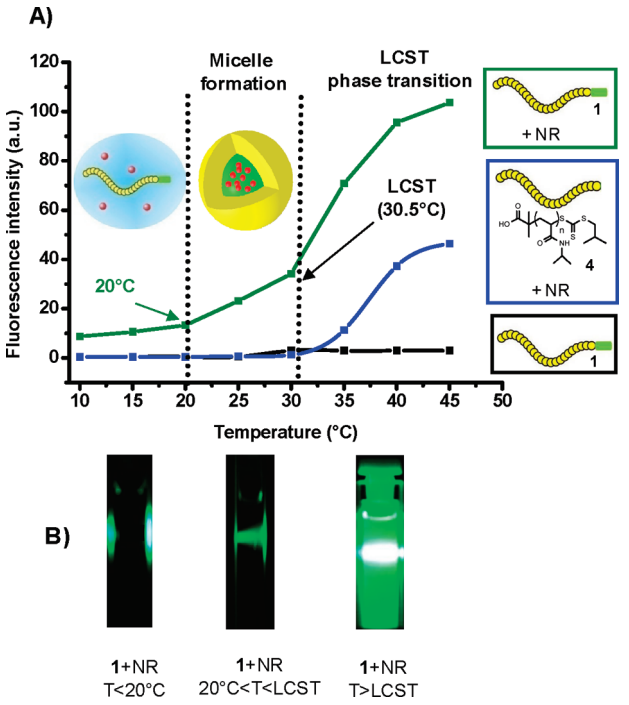

Figure 2. (A) Intensity of the fluorescence emission spectra of NR (red dot) recorded as a function of temperature in the presence of **1** (3 mg mL^{-1}, green curve) or **4** (3 mg mL^{-1}, blue curve) in aqueous solution. Fluorescence intensity of **1** (3 mg mL^{-1}, dark curve) vs temperature in aqueous solution. λ_{ex} = 530 nm. λ_{em} = 625 nm. (B) Photographs showing the fluorescence of an aqueous solution of **1**+NR at $T < 20$ °C, (left), 20 °C < T < LCST (middle) and at $T >$ LCST (right).

Figure 2 shows the dependence of the relative fluorescence intensity of NR as a function of temperature in the presence of **1** and control polymer **4** (M_n = 8100 g mol^{-1}, PDI = 1.13) which does not incorporate a TTF unit. For both polymers at low temperatures (<20 °C), the fluorescence emission intensity of NR was very low suggesting that the dye was not located in a hydrophobic environment and thereby indicating that **1** and **4** did not form micelles under these conditions. At higher temperature, the evolution of the fluorescence emission intensity of NR displayed different features. As the temperature increased, the fluorescence intensity of NR displayed two abrupt changes at 20 and 30 °C in the presence of **1**, indicating partitioning of the fluorescent probe into two different hydrophobic domains.[61,62] For polymer **4** only the second sharp variation in the fluorescence intensity appeared at around 30 °C. Hence, the presence of the TTF unit dictated the first hydrophobic microdomain formation.

In a recent investigations, we have examined by Cryo-TEM and DLS the size and morphology of **1** and **4** at 24 °C and we showed that while **1** formed a monomodal size distribution of individual spherical micelles (average micelle diameter = 26 nm), **4** existed as unimers.[54] Therefore, the first change observed at 20 °C in the fluorescence intensity of NR may originate from the unimer−micelle transition. At temperatures below 20 °C, **1** exists as unimers which then self-assembles upon heating, leading to the formation of the corresponding micelles. The second phase transition observed for both **1** and **4** was ascribed to the LCST phase transition since, at this temperature, the transparent solution underwent a characteristic abrupt change in turbidity due to the precipitation of the polymer. Moreover, the value of

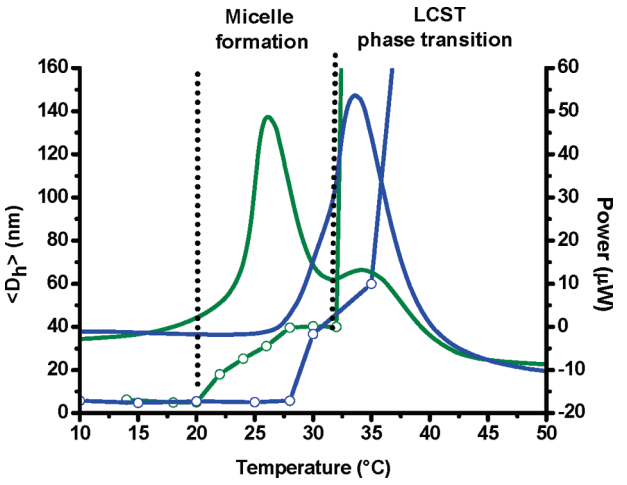

Figure 3. Apparent hydrodynamic diameter (D_h) of **1** (green circle) and **4** (blue circle) as a function of temperature (0.5 °C min^{-1}). DSC thermograms of polymer of **1** (green line) and **4** (blue line) (second heating scan at 0.5 °C min^{-1}). Concentration of polymers: 3 mg mL^{-1}.

the cloud point estimated from variable temperature fluorescence experiments was in good accordance with that obtained from UV−vis turbidity experiments (30.5 °C).[54] It should be noted that NR displayed a stronger fluorescence intensity above the LCST than between 20 °C < T < LCST. This confirms that strongly hydrophobic microenvironments are generated when thermo sensitive PNIPAM polymers reach their LCST.[63]

To further characterize the solution properties of **1** and **4**, we undertook variable-temperature-DLS and nano-DSC experiments. Figure 3 shows the temperature dependency of the hydrodynamic diameter (D_h) and the heat capacity during heating (0.5 °C min^{-1}) of 0.3 wt % solutions of **1** and **4**. Data obtained for both DLS and DSC techniques were consistent with fluorescence data. Indeed, DLS results showed two successive abrupt changes in the D_h and two endothermic transitions were detected by DSC for **1**. In particular, the first change at 20 °C estimated from fluorescence spectroscopy coincided both with the first abrupt change in the DLS signal and with the onset of the first endothermic phase transition peak. Furthermore, DSC results confirmed the key role played by the TTF unit in the unimer−micelle transition since polymer **4**, which did not bear the TTF unit, did not show the first endothermic transition upon heating. In this last case, only the second change in the apparent hydrodynamic diameter and the second endothermic phase transition corresponding to the LCST phase transition were observed by DLS and DSC, respectively.

Interestingly, the DSC analysis of polymer **1** proved that both steps are reversible, because successive scans were essentially identical (see Supporting Information, Figure S1). Moreover, the enthalpy for the micellization step was much larger (about 4.5 kJ mol^{-1}) than the enthalpy for the second step (about 1.5 kJ mol^{-1}). These values can be compared to the known transition enthalpy for PNIPAM LCST (4.6−7.1 kJ mol^{-1}),[64,65] which is related to the thermally induced dehydration of the polymer. In particular, the fact that enthalpy of the second step amounts to only one-fourth of the expected enthalpy for the PNIPAM LCST means that about only one-fourth of the NIPAM units in the system were dehydrated during the second step. In fact, it is well-known that the architecture of the polymer can have a strong influence on the transition temperature and enthalpy.[66] For

dx.doi.org/10.1021/ma2009854 |*Macromolecules* 2011, 44, 6532–6538

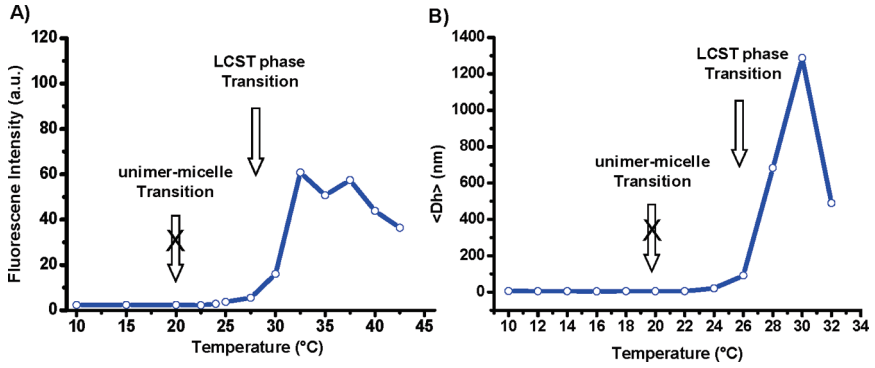

Figure 4. (A) Intensity of the fluorescence emission spectra of NR as a function of the temperature for complex **1.2** (3×10^{-4} M, λ_{ex} = 530 nm, λ_{em} = 625 nm). (B) Apparent hydrodynamic diameter (D_h) of **1.2** (3×10^{-4} M) recorded as a function of temperature.

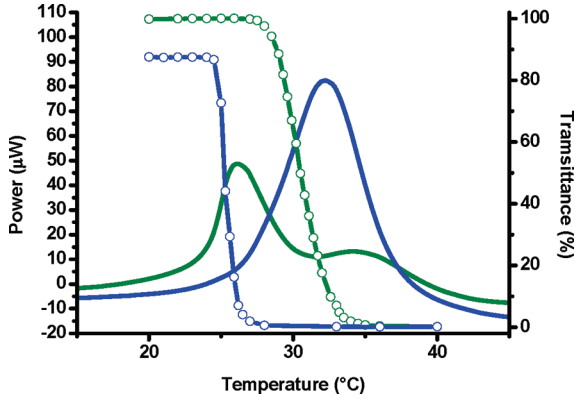

Figure 5. DSC thermograms of **1** (green line) and **1.2** (blue line) and transmittance vs temperature curves for **1** (green circle) and **1.2** (blue circle) at a concentration of 0.3 mM.

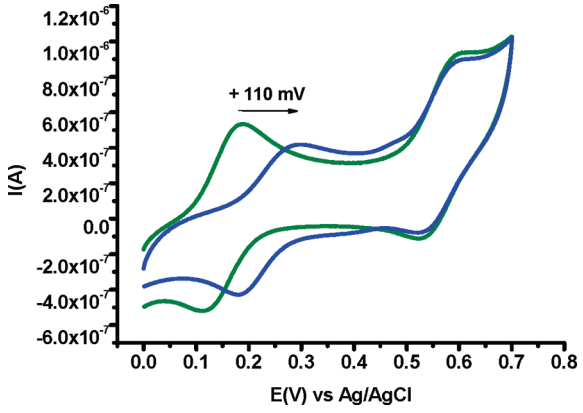

Figure 6. Cyclic voltammograms of **1** (green line) and upon the addition of 10 equiv of **3** (relative to **1**) (blue line) in 0.5 M NaCl/H_2O at scan rate =50 mV s^{-1}. Recorded at 15 °C using a platinium working electrode and an Ag/AgCl reference electrode.

example, branching,[67] cross-linking,[68] or adsorption on surfaces[69] limit the hydration of PNIPAM chains at low temperature and therefore reduces the amount of water released at the LCST. It is therefore tempting to propose the following model, where the first step associated with the micellization involves not only the packing of the hydrophobic TTF units, but also the partial dehydration of a large fraction (about 75%) of the PNIPAM chains. The portions of the chains which remain hydrated, probably cover and stabilize the micelles up to the LCST (second step), where they are eventually also dehydrated.

Having shown that **1** displayed in water two successive phase transitions corresponding to the unimer−micelle and the LCST phase transition, respectively, we next turned our attention to whether the unimer−micelle transition process of **1** could be controlled by forming host−guest complexes with either **2** or **3**. In a recent study, we have demonstrated by fluorescence spectroscopy, ^{1}H NMR and cryo-TEM that the addition of **2** to a solution containing micelles fabricated from **1** at 25 °C resulted in the disassembly of the latter and the release of preloaded NR due to the formation of a pseudorotaxane-like architecture. Here, the objective was to undertake a detailed investigation of the role complex-mediated modulation of the hydrophobicity of the TTF unit has on the unimer-to-micelle transition of **1**. For this purpose, we have first investigated the influence the formation of **1.2** has on the fluorescence intensity of NR and on the hydrodynamic diameter of **1** at different temperatures. As depicted in the Figure 4A, upon the addition of **2** to a solution of **1** the first abrupt change in emission intensity of NR disappeared. The same trends (Figure 4B) were observed regarding DLS experiments, which clearly revealed the absence of the first change in the hydrodynamic diameter at around 20 °C. Hence, these results suggest that complex formation strongly altered the amphiphilicity of **1** thereby controlling the unimer−micelle transition phase.

To confirm this finding, a nano-DSC experiment was carried out on **1** in the presence of **2**. Figure 5 shows upon the addition of **2**, the first endothermic phase transition corresponding to the self-assembly process disappeared, thereby further indicating the key role played by the TTF unit in determining the amphiphilicity of **1** and therefore the micellization process. DSC traces also revealed that the formation of **1.2** induced a shift of the LCST toward a lower temperature (∼26 °C). This result was in a good agreement with the LCST value obtained from UV−vis turbidity experiments and with similar previously described systems[25] suggesting that the hydrophilicity−hydrophobicity balance of the material was displaced toward a more hydrophobic structure, presumably due to the formation of a pseudorotaxane-like architecture.

As an alternative strategy for masking the amphilicity of **1**, we have investigated the capability of cyclodextrins to form host-complexes with TTF derivatives.[58] The complexation between **1** and **3** was first established by cyclic voltammetry by comparing

dx.doi.org/10.1021/ma2009854 |*Macromolecules* 2011, 44, 6532–6538

voltammograms of **1** alone and in the presence of excess **3** (Figure 6). The CV recorded in water for **1** gave rise to two reversible one-electron oxidation waves at $E^1_{1/2}$ = 0.15 V and $E^2_{1/2}$ = 0.55 V, corresponding to the two-step oxidation (TTF $\rightarrow$ $TTF^{\bullet+}$ $\rightarrow$ TTF^{2+}) of the TTF unit. Upon the addition of **3** a positive shift in the first oxidation wave was observed. This destabilization of the $TTF^{\bullet+}$ state, together with a lowering of the peak current for this oxidation wave (compared to free polymer **1**) is indicative of inclusion of the TTF unit within the cavity of the CD unit. Interestingly, the addition of **3** to the CV cell containing **1** had little effect on the half-wave potential for the TTF^{2+} redox wave, suggesting that complex **1.3** dethreads upon the formation of the $TTF^{\bullet+}$ state.

Host–guest binding was also investigated by isothermal titration microcalorimetry (ITC) (see Figure 7). ITC experiments show that addition of **3** to a dilute solution of **1** in water at 15 °C gives rise to an exothermic response (ΔH = −38.5 (±0.2) kJ mol^{-1}) consistent with 1:1 host–guest complexation (n_{exp} = 1.17). Analysis of the titration data gave an association constant (K_a) of 1.1 (±0.2) × 10^4 M^{-1} for **1.3**.

Next, to probe the effect complexation between **1** and **3** has in modulating the amphiphilicity and the self-assembly **1** in aqueous solution, we have undertaken nano-DSC experiments (Figure 8, green and blue curves). The addition of **3** resulted in the disappearance of the first endothermic transition in the DSC curve, characteristic of the unimer-micelle transition. Further evidence to prove that **3** was able to modulate the self-assembly of **1** was achieved by performing DLS experiments for **1** in the presence of **3** at various temperatures. Indeed, as shown in Figure 8B (green and blue curves), the data clearly revealed the absence of the first change in the apparent hydrodynamic diameter at 20 °C upon the addition of **3**, thus reinforcing the nano-DSC results which showed that complex formation resulted in the disruption of micelles.

As a strategy for disassembling pseudorotaxane **1.3** and thus for reforming micelles, we have explored the addition of 1-adamantanol to a solution of **1.3**, as it is established that adamantane derivatives are effective guests for cyclodextrin derivatives in water. We have determined the K_a for the complex of 1-adamantanol and RAMEB using ITC which gave a value of 1.4 × 10^4 M^{-1} (see Supporting Information, Figure S2). This slightly larger K_a value than that obtained for **1.3** suggests that the addition of an excess of 1-adamantanol may result in the dethreading of complex **1.3**. As depicted in Figure 8A (red curve), the addition of aliquots of 1-adamantanol to **1.3** resulted in the reappearance of the first endothermic peak corresponding to the micellization process in

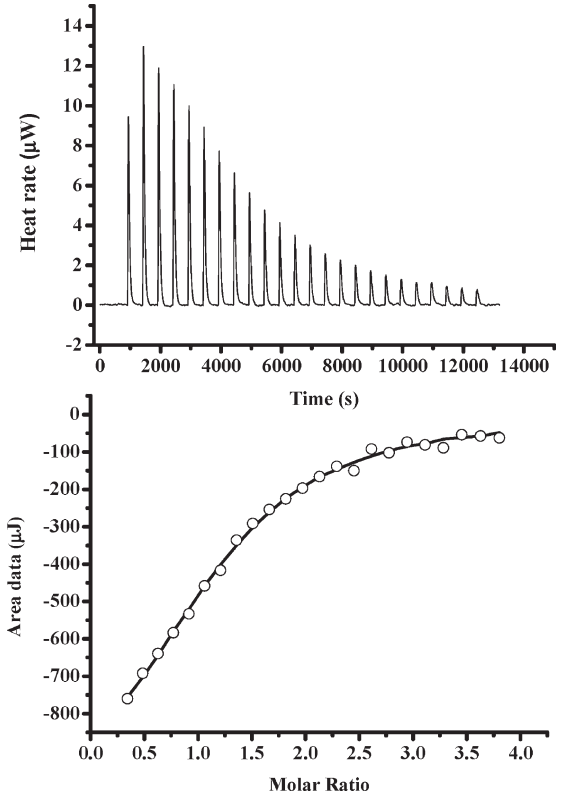

Figure 7. Isothermal titration calorimetry data for the addition of aliquots of **3** (3 mM) to **1** (0.2 mM). Recorded in H_2O at 15 °C.

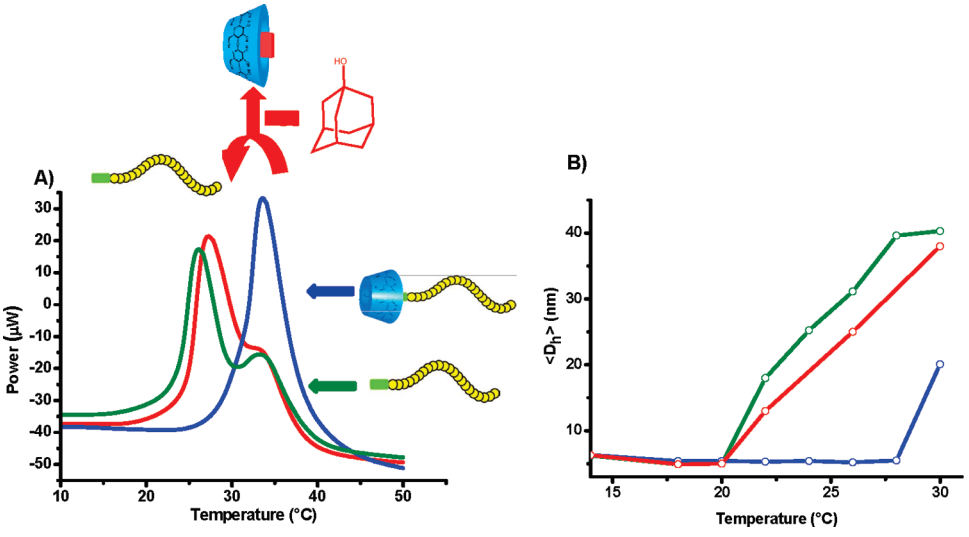

Figure 8. (A) DSC thermograms of polymer of **1** (green line) at a concentration of 0.3 mM, **1** + **3** (blue line) (4 equiv. compared to **1**), **1** + **3** + 1-adamantanol (red line) (20 equiv. compared to **1**) (0.5 °C min^{-1}). (B) Apparent hydrodynamic diameter (D_h) of **1** (green line), **1** + **3** (blue line) (4 equiv. compared to **1**), **1** + **3** + 1-adamantanol (red line) (20 equiv compared to **1**) as a function of temperature.

dx.doi.org/10.1021/ma2009854 |*Macromolecules* 2011, 44, 6532–6538

the nano-DSC trace. In control experiments, we have recorded DSC thermograms of **1** in the presence of 1-adamantanol (see Supporting Information, Figure S3). These experiments revealed that two successive endothermic phase transitions were observed that are similar to those observed for **1** alone. Thus, the DSC data are consistent with the 1-adamantanol disrupting complex formation between **1** and **3** and thus allowing the reformation of micelles of **1**. To further prove the ability of 1-adamantanol to disrupt supramolecular complex formation, we have investigated the change in the apparent hydrodynamic diameter of an admixture of **1** and **3** upon the addition of 1-adamantanol using DLS (Figure 8B, red curve). Indeed, in the presence of 1-adamantanol, DLS data clearly revealed the previously observed first change in the apparent hydrodynamic diameter of **1** is present, consistent with the unimer-micelle transition.

CONCLUSIONS

In summary, the present study has provided further understanding of the temperature-induced micellization of an amphiphilic linear end-functionalized TTF poly(*N*-isopropylacrylamide) in aqueous solution. The fluorescence, DLS and nano-DSC data suggest that this polymer underwent two successive phase transitions corresponding to the unimer-to-micelle and LCST transitions as the temperature is increased. Next we have shown that the amphiphilicity of **1** could be controlled by forming pseudorotaxane architectures with **2** or **3**. Cyclic voltammetry experiments revealed that the pseudorotaxane-like architecture **1.3** could be disassembled by oxidizing the TTF moiety. Furthermore, the complexation between **1** and **3** was also tunable by the addition of competing guest 1-adamantanol, which resulted in the reformation of micelles of **1**. Hence, the opportunity to control the micellization using temperature, electrochemistry and molecular recognition processes[54] paves the way for the construction of future switchable self-assembled systems with advanced materials and drug delivery applications.

ASSOCIATED CONTENT

Supporting Information. DSC thermograms of polymer **1**, isothermal titration calorimetry data, DSC thermogram of polymer **1** in the presence of 1-adamantanol. This material is available free of charge via the Internet at http://pubs.acs.org.

AUTHOR INFORMATION

Corresponding Author

*E-mail: (G.C.) Graeme.Cooke@glasgow.ac.uk; (P.W.) patrice.woisel@ensc-lille.fr .

ACKNOWLEDGMENT

P.W. and G.C. thank the Agence Nationale de la Recherche (ANR-09-JCJC-0032-01) and the EPRSC, respectively, for funding.

REFERENCES

(1) Brunsveld, L.; Folmer, B. J. B.; Meijer, E. W.; Sijbesma, R. P. *Chem. Rev.* **2001**, *101*, 4071–4098.
(2) Cordier, P.; Tournilhac, F.; Soulie-Ziakovic, C.; Leibler, L. *Nature* **2008**, *451*, 977–980.
(3) Harada, A.; Li, J.; Kamachi, M. *Nature* **1992**, *356*, 325–327.
(4) Hirschberg, J. H. K. K.; Brunsveld, L.; Ramzi, A.; Vekemans, J. A. J. M.; Sijbesma, R. P.; Meijer, E. W. *Nature* **2000**, *407*, 167–170.
(5) Raymo, F. M.; Stoddart, J. F. *Chem. Rev.* **1999**, *99*, 1643–1664.
(6) Shimizu, T.; Masuda, M.; Minamikawa, H. *Chem. Rev.* **2005**, *105*, 1401–1444.
(7) Olson, M. A.; Coskun, A.; Fang, L.; Basuray, A. N.; Stoddart, J. F. *Angew. Chem., Int. Ed.* **2010**, *49*, 3151–3156.
(8) Chen, Y.; Dong, C.-M. *J. Phys. Chem. B* **2010**, *114*, 7461–7468.
(9) Bouteiller, L. Assembly via Hydrogen Bonds of Low Molar Mass Compounds into Supramolecular Polymers. In *Hydrogen Bonded Polymers*; Binder, W., Ed.; Springer: Berlin/Heidelberg: 2007; Vol. 207, pp 79−112.
(10) Zhang, J.; Sun, H.; Ma, P. X. *ACS Nano* **2010**, *4*, 1049–1059.
(11) Han, J.; Gao, C. *Curr. Org. Chem.* **2011**, *15*, 2–26.
(12) Weck, M. *Polym. Int.* **2007**, *56*, 453–460.
(13) Folmer, B. J. B.; Sijbesma, R. P.; Versteegen, R. M.; van der Rijt, J. A. J.; Meijer, E. W. *Adv. Mater.* **2000**, *12*, 874–878.
(14) South, C. R.; Weck, M. *Macromolecules* **2007**, *40*, 1386–1394.
(15) Beck, J. B.; Rowan, S. J. *J. Am. Chem. Soc.* **2003**, *125*, 13922–13923.
(16) Reczek, J. J.; Kennedy, A. A.; Halbert, B. T.; Urbach, A. R. *J. Am. Chem. Soc.* **2009**, *131*, 2408–2415.
(17) Bria, M.; Bigot, J.; Cooke, G.; Lyskawa, J.; Rabani, G.; Rotello, V. M.; Woisel, P. *Tetrahedron* **2009**, *65*, 400–407.
(18) Chen, L.; Zhu, X.; Yan, D.; Chen, Y.; Chen, Q.; Yao, Y. *Angew. Chem., Int. Ed.* **2006**, *45*, 87–90.
(19) Sakai, R.; Otsuka, I.; Satoh, T.; Kakuchi, R.; Kaga, H.; Kakuchi, T. *Macromolecules* **2006**, *39*, 4032–4037.
(20) Leung, K. C. F.; Mendes, P. M.; Magonov, S. N.; Northrop, B. H.; Kim, S.; Patel, K.; Flood, A. H.; Tseng, H.-R.; Stoddart, J. F. *J. Am. Chem. Soc.* **2006**, *128*, 10707–10715.
(21) Huang, F.; Nagvekar, D. S.; Slebodnick, C.; Gibson, H. W. *J. Am. Chem. Soc.* **2005**, *127*, 484–485.
(22) Messing, R.; Schmidt, A. M. *Polym. Chem.* **2011**, *2*, 18–32.
(23) Appel, E. A.; Biedermann, F.; Rauwald, U.; Jones, S. T.; Zayed, J. M.; Scherman, O. A. *J. Am. Chem. Soc.* **2010**, *132*, 14251–14260.
(24) Kretschmann, O.; Steffens, C.; Ritter, H. *Angew. Chem., Int. Ed.* **2007**, *46*, 2708–2711.
(25) Bigot, J.; Fournier, D.; Lyskawa, J.; Marmin, T.; Cazaux, F.; Cooke, G.; Woisel, P. *Polym. Chem.* **2010**, *1*, 1024–1029.
(26) Harada, A.; Kobayashi, R.; Takashima, Y.; Hashidzume, A.; Yamaguchi, H. *Nat Chem* **2011**, *3*, 34–37.
(27) Liao, X.; Chen, G.; Liu, X.; Chen, W.; Chen, F.; Jiang, M. *Angew. Chem., Int. Ed.* **2010**, *49*, 4409–4413.
(28) Cooke, G.; Garety, J. F.; Hewage, S. G.; Jordan, B. J.; Rabani, G.; Rotello, V. M.; Woisel, P. *Org. Lett.* **2007**, *9*, 481–484.
(29) Wang, Z.; Feng, Z.; Gao, C. *Chem. Mater.* **2008**, *20*, 4194–4199.
(30) Zhang, W.; DeIonno, E.; Dichtel, W. R.; Fang, L.; Trabolsi, A.; Olsen, J.-C.; Benitez, D.; Heath, J. R.; Stoddart, J. F. *J. Mater. Chem.* **2011**, *21*, 1487–1495.
(31) Schatz, C.; Louguet, S.; Le Meins, J.-F.; Lecommandoux, S. *Angew. Chem., Int. Ed.* **2009**, *48*, 2572–2575.
(32) Lutz, J.-F. *Polym. Int.* **2006**, *55*, 979–993.
(33) McCormick, C. L.; Sumerlin, B. S.; Lokitz, B. S.; Stempka, J. E. *Soft Matter* **2008**, *4*, 1760–1773.
(34) Riess, G. *Prog. Polym. Sci.* **2003**, *28*, 1107–1170.
(35) Smith, A. E.; Xu, X.; McCormick, C. L. *Prog. Polym. Sci.* **2010**, *35*, 45–93.
(36) Rapoport, N. *Prog. Polym. Sci.* **2007**, *32*, 962–990.
(37) Wei, H.; Cheng, S.-X.; Zhang, X.-Z.; Zhuo, R.-X. *Prog. Polym. Sci.* **2009**, *34*, 893–910.
(38) Ganta, S.; Devalapally, H.; Shahiwala, A.; Amiji, M. *J. Controlled Release* **2008**, *126*, 187–204.
(39) Stenzel, M. H. *Chem. Commun.* **2008**, 3486–3503.
(40) Meng, F.; Zhong, Z.; Feijen, J. *Biomacromolecules* **2009**, *10*, 197–209.
(41) Vriezema, D. M.; Aragonès, M. C.; Elemans, J. A. A. W.; Cornelissen, J. J. L. M.; Rowan, A. E.; Nolte, R. J. M. *Chem. Rev.* **2005**, *105*, 1445–1490.
(42) Schlütter, F.; Pavlov, G. M.; Gohy, J.-F.; Winter, A.; Wild, A.; Hager, M. D.; Hoeppener, S.; Schubert, U. S. *J. Polym. Sci., Part A: Polym. Chem.* **2011**, *49*, 1396–1408.

(43) Mugemana, C.; Guillet, P.; Hoeppener, S.; Schubert, U. S.; Fustin, C.-A.; Gohy, J.-F. *Chem. Commun.* **2010**, *46*, 1296–1298.
(44) Dong, H.; Li, Y.; Cai, S.; Zhuo, R.; Zhang, X.; Liu, L. *Angew. Chem., Int. Ed.* **2008**, *47*, 5573–5576.
(45) Chen, Y.; Pang, X.-H.; Dong, C.-M. *Adv. Funct. Mater.* **2010**, *20*, 579–586.
(46) Cho, S. Y.; Allcock, H. R. *Macromolecules* **2009**, *42*, 4484–4490.
(47) Liu, H.; Zhang, Y.; Hu, J.; Li, C.; Liu, S. *Macromol. Chem. Phys.* **2009**, *210*, 2125–2137.
(48) Joseph, J.; Dreiss, C. A.; Cosgrove, T.; Pedersen, J. S. *Langmuir* **2007**, *23*, 460–466.
(49) Zhang, Z.-X.; Liu, X.; Xu, F. J.; Loh, X. J.; Kang, E.-T.; Neoh, K.-G.; Li, J. *Macromolecules* **2008**, *41*, 5967–5970.
(50) Zhang, Z.-X.; Liu, K. L.; Li, J. *Macromolecules* **2011**, *44*, 1182–1193.
(51) Zou, J.; Guan, B.; Liao, X.; Jiang, M.; Tao, F. *Macromolecules* **2009**, *42*, 7465–7473.
(52) Zeng, J.; Shi, K.; Zhang, Y.; Sun, X.; Zhang, B. *Chem. Commun.* **2008**, 3753–3755.
(53) Yan, Q.; Yuan, J.; Cai, Z.; Xin, Y.; Kang, Y.; Yin, Y. *J. Am. Chem. Soc.* **2010**, *132*, 9268–9270.
(54) Bigot, J.; Charleux, B.; Cooke, G.; Delattre, F.; Fournier, D.; Lyskawa, J.; Sambe, L.; Stoffelbach, F.; Woisel, P. *J. Am. Chem. Soc.* **2010**, *132*, 10796–10801.
(55) Ashton, P. R.; Balzani, V.; Becher, J.; Credi, A.; Fyfe, M. C. T.; Mattersteig, G.; Menzer, S.; Nielsen, M. B.; Raymo, F. M.; Stoddart, J. F.; Venturi, M.; White, A. J. P.; Williams, D. J. *J. Am. Chem. Soc.* **1999**, *121*, 3951–3957.
(56) Devonport, W.; Blower, M. A.; Bryce, M. R.; Goldenberg, L. M. *J. Org. Chem.* **1997**, *62*, 885–887.
(57) Bigot, J.; Charleux, B.; Cooke, G.; Delattre, F.; Fournier, D.; Lyskawa, J.; Stoffelbach, F.; Woisel, P. *Macromolecules* **2009**, *43*, 82–90.
(58) Zhao, Y.-L.; Dichtel, W. R.; Trabolsi, A.; Saha, S.; Aprahamian, I.; Stoddart, J. F. *J. Am. Chem. Soc.* **2008**, *130*, 11294–11296.
(59) Odell, B.; Reddington, M. V.; Slawin, A. M. Z.; Spencer, N.; Stoddart, J. F.; Williams, D. J. *Angew. Chem., Int. Ed. Engl.* **1988**, *27*, 1547–1550.
(60) Bigot, J.; Bria, M.; Caldwell, S. T.; Cazaux, F.; Cooper, A.; Charleux, B.; Cooke, G.; Fitzpatrick, B.; Fournier, D.; Lyskawa, J.; Nutley, M.; Stoffelbach, F.; Woisel, P. *Chem. Commun.* **2009**, 5266–5268.
(61) Winnik, F. M. *Macromolecules* **1990**, *23*, 233–242.
(62) Akiyoshi, K.; Kang, E.-C.; Kurumada, S.; Sunamoto, J.; Principi, T.; Winnik, F. M. *Macromolecules* **2000**, *33*, 3244–3249.
(63) Fujimoto, K.; Nakajima, Y.; Kashiwabara, M.; Kawaguchi, H. *Polym. Int.* **1993**, *30*, 237–241.
(64) Schild, H. G.; Tirrell, D. A. *J. Phys. Chem.* **1990**, *94*, 4352–4356.
(65) Otake, K.; Inomata, H.; Konno, M.; Saito, S. *Macromolecules* **1990**, *23*, 283–289.
(66) Qiu, X.-P.; Winnik, F. M. *Macromol. Symp.* **2009**, *278*, 10–13.
(67) Haba, Y.; Kojima, C.; Harada, A.; Kono, K. *Angew. Chem.* **2007**, *46*, 234–237.
(68) Keerl, M.; Smirnovas, V.; Winter, R.; Richtering, W. *Macromolecules* **2008**, *41*, 6830–6836.
(69) Petit, L.; Bouteiller, L.; Brûlet, A.; Lafuma, F.; Hourdet, D. *Langmuir* **2007**, *23*, 147–158.